CHEMISTRY OF MATERIALS
Article

Chem. Mater. **2011,** *23,* 95–105 95
DOI:10.1021/cm102343r

Structural Variations on Self-Assembly and Macroscopic Properties of 1,4,5,8-Naphthalene-diimide Chromophores

Mijanur Rahaman Molla and Suhrit Ghosh*

Polymer Science Unit, Indian Association for the Cultivation of Science, 2A & 2B Raja S. C. Mullick Road, Kolkata 700032, India

Received August 16, 2010. Revised Manuscript Received October 27, 2010

Supramolecular assembly and macroscopic properties of a series of bis-(trialkoxybenzamide)-functionalized naphthalene-tetracarboxylicacid-diimide (NDI) chromophores have been studied. The number of methylene units (0, 2, 3, 4; **NDI-0**, **NDI-2**, **NDI-3**, **NDI-4**, respectively) in between the NDI chromophore and the amide functionalities have been systematically varied to understand the effect of this simple structural variations on the self-assembly. UV−visible spectroscopic studies revealed facile self-assembly in nonpolar medium by synergistic effect of π-stacking, hydrogen-bonding, and hydrophobic interactions. The propensity toward self-assembly was found to follow the order **NDI-0** $\gg$ **NDI-2** $\approx$ **NDI-3** $>$ **NDI-4** ,which could be attributed to the difference in strength of the H-bonding interaction. Atomic force microscopy (AFM) studies revealed unique morphology for the self-assembled structure in each case such as nanostructure with short-range order (**NDI-0**), elongated nanowires (**NDI-2**), relatively flat nanoribbons (**NDI-3**), and discontinuous nanofibers (**NDI-4**). Effect of such diverse morphologies was found to be highly relevant in correlating the macroscopic properties such as gelation of the individual chromophore. Most strongly aggregating **NDI-0** did not show gelation in any of the tested solvents but formed lyotropic mesophases (chromonic N and M- phase) which could be related to their crystal like morphology as revealed by AFM images. Contrary to this, **NDI-2** and **NDI-3** showed most promising gelation ability in many common organic solvents with very low critical gelation concentrations (in some cases even <0.1 wt %) and **NDI-4** formed gel only in few solvents which can be attributed to the strength of the self-assembly. The viscoelastic properties of the gels were studied by rheological measurements which revealed remarkable dependence on the morphology of the self-assembled structure. For example, although the self-assembly propensity and gelation ability were almost similar between **NDI-2** and **NDI-3**, the yield-stress of the former gel was estimated to be astonishingly high ($\sim$20 times) compared to that of **NDI-3** gel owing to the large differences in the aspect ratio of the respective 1D-nanostructures. Further the thermodynamic parameters such as ΔH_m (enthalpy of melting) of the gel-to-sol transition were determined for various gels and correlated with the molecular structure and self-assembly propensity in solution.

Introduction

The motivation to study supramolecular organization of various functional π-systems[1] stems from the desire to gain precise control over their interchromophoric interaction and resulting photophysical properties, which are highly relevant in the context of their utility in organic-electronic device applications.[2] In this context, appropriate molecular design to achieve long-range order in the self-assembled structure of the functional chromophore is extremely important because it will provide the desired continuous pathway for better transport of the charge-career mobilities.[3] Formation of such fibers with long-range ordering are often seen in organogels[4] generated from self-assembly of small-molecular building blocks. Gelation of building blocks with diverse nature has been studied with great interest in the recent past because of their potential applications in various disciplines ranging from chemistry to biology to materials sciences. A subclass of these gelators that consists of various p- and n-type semiconductors as

*Corresponding author. E-mail: psusg2@iacs.res.in.

(1) (a) *Supramolecular Dye Chemistry*; Würthner, F., Ed.; Topics in Current Chemistry; Springer: Berlin, Germany, 2005; Vol. *258*. (b) Palmer, L. C.; Stupp, S. I. *Acc. Chem. Res.* **2008**, *41*, 1674. (c) D'Souza, F.; Ito, O. *Chem. Commun.* **2009**, 4913. (d) Malinovskii, V. L.; Wenger, D.; Häner, R. *Chem. Soc. Rev.* **2010**, *39*, 410.

(2) (a) Hains, A. W.; Liang, Z.; Woodhouse, M. A.; Gregg, B. A. *Chem. Rev.* **2010**, *110*, 6689–6735 and references therein.

(3) (a) Warman, J. M.; De Haas, M. P.; Dicker, G.; Grozema, F. C.; Piris, J.; Debije, M. G. *Chem. Mater.* **2004**, *16*, 4600. (b) Warman, J. M.; Van de Craats, A. M. *Mol. Cryst. Liq. Cryst.* **2003**, *396*, 41. (c) Schoonbeek, F. S.; Van Esch, J. H.; Wegewijs, B.; Rep, D. B. A.; De Haas, M. P.; Klapwijk, T. M.; Kellogg, R. M.; Feringa, B. L. *Angew. Chem., Int. Ed.* **1999**, *38*, 1393. (d) Prasanthkumar, S.; Saeki, A.; Seki, S.; Ajayaghosh, A. *J. Am. Chem. Soc.* **2010**, *132*, 8866. (e) Chen, J.; Cheng, F. *Acc. Chem. Res.* **2009**, *42*, 713. (f) Cademartiri, L.; Ozin, G. A. *Adv. Mater.* **2009**, *21*, 1013.

(4) (a) Melendez, R. E.; Carr, A. J.; Linton, B. R.; Hamilton, A. D. *Struct. Bonding* (*Berlin*) **2000**, 31. (b) Laurent, H. B.; Desvergne, J. P. *Molecular Gels: Materials with Self-Assembled Fibrillar Networks*; Weiss, R. G.; Terech, P., Eds.; Springer: Dordrecht, The Netherlands, 2006; Chapter 12. (c) Beginn, U. *Prog. Polym. Sci.* **2003**, *28*, 1049. (d) Banerjee, S.; Das, R. K.; Maitra, U. *J. Mater. Chem.* **2009**, *19*, 6649. (e) Dastidar, P. *Chem. Soc. Rev.* **2008**, *37*, 2699.

Published on Web 12/09/2010

Scheme 1. Schematic Representation of a Commonly Utilized Molecular Design for Selfassembly of Various Functional π-Systems

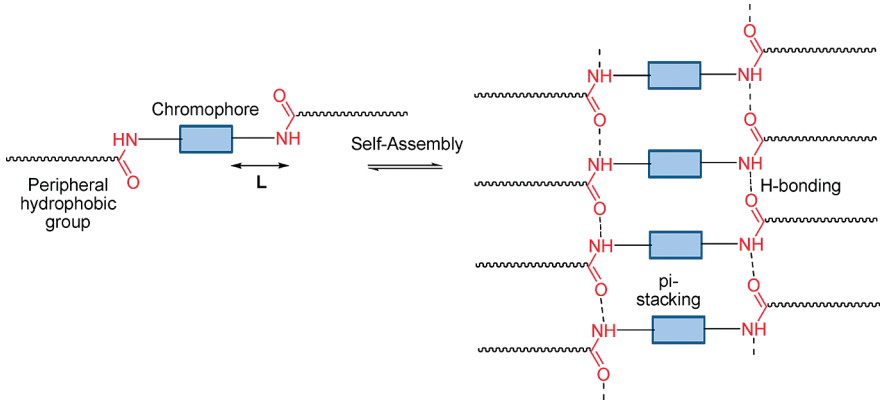

the small-molecular building block has generated tremendous enthusiasm in the forgone decade because of their exciting photophysical properties[5] in the gel state, which opens up the possibility of utilizing them as active materials in devices such as bulk-heterojunction solar-cells, organic thin-film transistors etc.[6] Examples of such building blocks include various functional π-systems such as oligo-phenylenevinylene,[7] oligo-phenyleneethynylene,[8] oligo-thienylenevinylene,[3c] phthalocyanine,[9] porphyrin,[10] oligothiophene,[11] tetrathiofulvalene,[12] perylene-diimide,[13] naphthalene-diimide,[14] merocyanines,[15] etc. Unlike other systems, these building blocks provide the added advantage of examining the self-assembly phenomenon independently in dilute solutions by monitoring their photophysical properties with various spectroscopic techniques and thus the possibility of correlating the molecular level interaction with the macroscopic properties such as gelation can be explored. We envisaged that such structure−property relationship studies[16] will be highly desirable to realize the scope as well as the limitations of structural modifications in the molecular level to achieve the desired macroscopic property. If one takes an account of the recent literature related to this field,[6−15] it will be evident that in most cases the molecular design for the functional building block is conceptually similar which is depicted in Scheme 1. The desired π-system is functionalized with peripheral hydrophobic groups which are linked to the chromophore with an amide or urea functional groups. Self-assembly in such systems is facilitated by the synergistic effect of π-stacking and hydrogen-bonding and the presence of hydrophobic peripheral functionalities provides the opportunity to study the self-assembly in nonpolar medium where hydrogen-bonding can be most influential. We are particularly interested in studying the effect of the distance of the hydrogen bonding functionalities with respect to the chromophore ("L" in Scheme 1)[17] in the self-assembly and gelation phenomenon. To realize this effect, we have

(5) (a) Hoeben, F. J. M.; Jonkheijm, P.; Meijer, E. W.; Schenning, A. P. H. J. *Chem. Rev.* **2005**, *105*, 1491. (b) Bhattacharya, S.; Samanta, S. K. *Langmuir* **2009**, *25*, 8378.

(6) (a) Brédas, J.-L.; Norton, J. E.; Cornil, J.; Coropceanu, V. *Acc. Chem. Res.* **2009**, *42*, 1691. (b) Amabilino, D. B.; P-L., J. *Soft Matter* **2010**, *6*, 1605. (c) Schmidt-Mende, L.; Fechtenkötter, A.; Muüllen, K; Moons, E.; Friend, R. H.; MacKenzie, J. D. *Science* **2001**, *293*, 1119. (d) Tang, C. W. *Appl. Phys. Lett.* **1986**, *48*, 183. (e) Dimitrakopoulos, C. D.; Malenfant, P. R. L. *Adv. Mater.* **2002**, *14*, 99. (f) Jones, B. A.; Ahrens, M. J.; Yoon, M. H.; Facchetti, A.; Marks, T. J.; Wasielewski, M. R. *Angew. Chem., Int. Ed.* **2004**, *43*, 6363. (g) Schmidt, R.; Ling, M. M.; Winkler, J. H.; Oh, M.; Könemann, M.; Bao, Z.; Würthner, F. *Adv. Mater.* **2007**, *19*, 3692. (h) Fernández, G.; Sánchez, L.; Veldman, D.; Wienk, M. M.; Atienza, C.; Guldi, D. M.; Janssen, R. A. J.; Martín, N. *J. Org. Chem.* **2008**, *73*, 3189. (i) Wohrle, D.; Kreienhoop, L.; Schnurpfeil, G.; Elbe, J.; Tennigkeit, B.; Hiller, S.; Schlettweinb, D. *J. Mater.Chem.* **1995**, *5*, 1819. (j) Wicklein, A.; Ghosh, S.; Sommer, M.; Würthner, F.; Thelakkat, M. *ACS Nano* **2009**, *3*, 1107.

(7) Ajayaghosh, A.; Praveen, V. K. *Acc. Chem. Res.* **2007**, *40*, 644and references therein.

(8) (a) Ajayaghosh, A.; Varghese, R.; Praveen, V. K.; Mahesh, S. *Angew. Chem., Int. Ed.* **2006**, *45*, 3261. (b) Ajayaghosh, A.; Varghese, R.; Mahesh, S.; Praveen, V. K. *Angew. Chem., Int. Ed.* **2006**, *45*, 7729.

(9) Engelkamp, H.; Middelbeek, S.; Nolte, R. J. M. *Science* **1999**, *284*, 785.

(10) (a) Tamaru, S. I.; Nakamura, M.; Takeuchi, M.; Shinkai, S. *Org. Lett.* **2001**, *3*, 3631. (b) Shirakawa, M.; Kawano, S. I.; Fujita, N.; Sada, K.; Shinkai, S. *J. Org. Chem.* **2003**, *68*, 5037.

(11) (a) Mishra, A.; Ma, C.-Q.; Bauerle, P. *Chem. Rev.* **2009**, *109*, 1141. (b) Schoonbeek, F. S.; Van Esch, J. H.; Wegewijs, B.; Rep, D. B. A.; De Haas, M. P.; Klapwijk, T. M.; Kellogg, R. M.; Feringa, B. L. *Angew. Chem., Int. Ed.* **1999**, *38*, 1393. (c) Kawano, S.; Fujita, N.; Shinkai, S. *Chem.—Eur. J.* **2005**, *11*, 4735.

(12) (a) Puigmartí-Luis, J.; Pino, Á. P.; Laukhin, V.; Feldborg, L. N.; Rovira, C.; Laukhina, E.; Amabilino, D. B. *J. Mater. Chem.* **2010**, *20*, 466. (b) Puigmartí-Luis, J.; Laukhin, V.; Pino, Á. P.; V-Gancedo, J.; Rovira, C.; Laukhina, E.; Amabilino, D. B. *Angew. Chem., Int. Ed.* **2007**, *46*, 238. (c) Akutagawa, T.; Kakiuchi, K.; Hasegawa, T.; Noro, S-i.; Nakamura, T.; Hasegawa, H.; Mashiko, S.; Becher, J. *Angew. Chem., Int. Ed.* **2005**, *44*, 7283.

(13) (a) Würthner, F. *Chem. Commun.* **2004**, 1564. (b) Sugiyasu, K.; Fujita, N.; Shinkai, S. *Angew. Chem., Int. Ed.* **2004**, *43*, 1229. (c) Li, X.-Q.; Stepanenko, V.; Chen, Z.; Prins, P.; Siebbeles, L. D. A.; Würthner, F. *Chem. Commun.* **2006**, 3871. (d) Würthner, F.; Bauer, C.; Stepanenko, V.; Yagai, S. *Adv. Mater.* **2008**, *20*, 1695.

(14) Mukhopadhyay, P.; Iwashita, Y.; Shirakawa, M.; Kawano, S-i.; Fujita, N.; Shinkai, S. *Angew. Chem., Int. Ed.* **2006**, *45*, 1592.

(15) (a) Würthner, F.; Yao, S.; Beginn, U. *Angew. Chem., Int. Ed.* **2003**, *42*, 3247. (b) Yagai, S.; Ishii, M.; Karatsu, T.; Kitamura, A. *Angew. Chem., Int. Ed.* **2007**, *46*, 8005.

(16) For few recent reports on structure−property relationship studies in the context of self-assembly of various functional π-systems see: (a) Ghosh, S.; Li, X.-Q.; Stepanenko, V.; Würthner, F. *Chem.—Eur. J.* **2008**, *14*, 11343. (b) Kaiser, T. K.; Stepanenko, V.; Würthner, F. *J. Am. Chem. Soc.* **2009**, *131*, 6719. (c) Yagai, S.; Kubota, S.; Iwashima, T.; Kishikawa, K.; Nakanishi, T.; Karatsu, T.; Kitamura, A. *Chem.—Eur. J.* **2008**, *14*, 5246. (d) Samanta, S. K.; Pal, A.; Bhattacharya, S. *Langmuir* **2009**, *25*, 8567. (e) Wicklein, A.; Lang, A.; Muth, M. A.; Thelakkat, M. *J. Am. Chem. Soc.* **2009**, *131*, 14442. (f) Jancy, B.; Asha, S. K. *Chem. Mater.* **2008**, *20*, 169. (g) Jancy, B.; Asha, S. K. *J. Phys. Chem. B.* **2006**, *110*, 20937.

(17) For a very recent report regarding significant effect on self-assembly due to such structural variation see: Miyajima, D.; Araoka, F.; Takezoe, H.; Kim, J.; Kato, K.; Takata, M.; Aida, T. *J. Am. Chem. Soc.* **2010**, *132*, 8530–8531.

studied the self-assembly and gelation of a series of structurally related naphthalene-tetracarboxylicacid-diimide (NDI)[18,19] chromophores because of their tremendous potential as n-type semiconducting materials[20] in various organic electronic devices.[21] These chromophores have also been utilized extensively to construct various elegant supramolecular structures such as foldamers,[22] organogels,[23] as well as hydrogels,[24] catenanes,[25] rotaxanes,[26] synthetic ion channels,[27] various supramolecular photosystems,[28] etc. Recently we have demonstrated a novel approach for self-sorted assembly of donor and acceptor chromophores wherein we used NDI as the acceptor unit.[29] Thus we envisaged that tuning the self-assembly and photophysical properties of this very important chromophore will be useful for better understanding of various exciting future new soft-materials. The structures of various NDI π-systems studied in this report are shown in Scheme 2. We have systematically varied the number of methylene groups in between the NDI chromophore and

Scheme 2. Structure of Various NDI Derivatives Studied in This Report

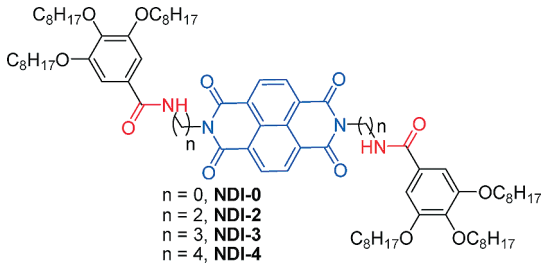

the amide functionality and studied the effect of this simple structural variation on the self-assembly of the respective chromophore. In this paper, we reveal the astonishing effect of this rather small structural variations on the self-assembly and also how the difference in mode and strength of self-assembly in solution was reflected in the morphology of the resulting nanostructures. Further, we examined the effect of these versatile morphologies on the next-level assembly of the chromophores such as lyotropic mesophases or gelation and correlated the rheological properties of these highly attractive soft materials with the morphology of the self-assembled nanostructures.

Results and Discussion

Spectroscopic Studies to Probe the Self-Assembly. Synthesis of various NDI chromophores reported in this paper was achieved using standard protocol.[30] The self-assembly of each system was studied independently by solvent-dependent UV−visible experiments. Chloroform is known to be good solvent for rigid π-systems, whereas aliphatic nonpolar solvent like methylcyclohexane (MCH) favors both π-stacking and hydrogen bonding. Thus to monitor the evolution of self-assembled structure from monomeric chromophore, the solvent composition was systematically varied from $CHCl_3$ to MCH keeping the concentration of the chromophore fixed at 0.1 mM. The solvent-dependent UV−visible data for the four NDI chromophores are presented in Figure 1. For every system, very similar well-resolved spectra were noticed in $CHCl_3$ in the range of 300−400 nm due to $\pi-\pi^*$ transition polarized along the long axis of the monomeric NDI chromophores. Going from $CHCl_3$ to MCH/$CHCl_3$ (95:5), the spectral pattern changed drastically with distinctly different characteristics depending upon the individual system. For all of them, significant hypochromic shift (~50−60%) was observed for all the major bands with concomitant bathochromic shift as suggested by the appearance of absorbance band beyond 400 nm. Also there was red-shift (2, 3, and 8 nm, respectively, for the **NDI-0**, **NDI-2**, and **NDI-3**) of the lowest energy absorption band at ~380. These results indicate formation of J-type assembly[31] with longitudinal displacement along the long axis of the chromophores. To compare the relative propensities for self-assembly in these four systems we monitored the intensity of the newly appeared

(18) For a recent review on core-unsubstituted NDI systems see: Bhosale, S. V.; Jani, C. H.; Langford, S. J. *Chem. Soc. Rev.* **2008**, *37*, 331.
(19) For a comprehensive review on the most recent advancement with core-substituted NDI see: Sakai, N.; Mareda, J.; Vauthey, E.; Matile, S. *Chem. Commun.* **2010**, *46*, 4225.
(20) (a) Miller, L. L.; Mann, K. R. *Acc. Chem. Res.* **1996**, *29*, 417. (b) Katz, H. E.; Lovinger, A. J.; Johnson, J.; Kloc., C.; Siegrist, T.; Li, W.; Lin, Y. Y.; Dodabalapur, A. *Nature* **2000**, *404*, 478. (c) Warman, J. M.; de Haas, M. P.; Dicker, G.; Grozema, F. C.; Piris, J.; Debije, M. G. *Chem. Mater.* **2004**, *16*, 4600. (d) Jones, B. A.; Facchetti, A.; Wasielewski, M. R.; Marks, T. J. *J. Am. Chem. Soc.* **2007**, *129*, 15259.
(21) (a) Oh, B. J. H.; Suraru, S. L.; Lee, W. Y.; Könemann, M.; Höffken, H. W.; Röger, C.; Schmidt, R.; Chung, Y.; Chen, W. C.; Würthner, F.; Bao, Z. *Adv. Funct. Mater.* **2010**, *20*, 2148. (b) Wei, Y.; Zhang, Q.; Jiang, Y.; Yu, J. *Macromol. Chem. Phys.* **2009**, *210*, 769.
(22) (a) Lokey, R. S.; Iverson, B. L. *Nature* **1995**, *375*, 303. (b) Nguyen, J. Q.; Iverson, B. L. *J. Am. Chem. Soc.* **1999**, *121*, 2639. (c) Zych, A. J.; Iverson, B. L. *J. Am. Chem. Soc.* **2000**, *122*, 8898. (d) Gabriel, G. J.; Iverson, B. L. *J. Am. Chem. Soc.* **2002**, *124*, 15174. (e) Cubberley, M. S.; Iverson, B. L. *J. Am. Chem. Soc.* **2001**, *123*, 7560.
(23) Mukhopadhyay, P.; Iwashita, Y.; Shirakawa, M.; Kawano, S-i.; Fujita, N.; Shinkai, S. *Angew. Chem., Int. Ed.* **2006**, *45*, 1592.
(24) (a) Shao, H.; Nguyen, T.; Romano, N. C.; Modarelli, D. A.; Parquette, J. R. *J. Am. Chem. Soc.* **2009**, *131*, 16374. (b) Shao, H.; Parquette, J. R. *Chem. Commun.* **2010**, *46*, 4285.
(25) (a) Au-Yeung, H. Y.; Pantos, G. D.; Sanders, J. K. M. *Angew. Chem., Int. Ed.* **2010**, *49*, 5331. (b) Au-Yeung, H. Y.; Pantos, G. D.; Sanders, J. K. M. *Proc. Natl. Acad. Sci. U.S.A.* **2009**, *106*, 10466. (c) Au-Yeung, H. Y.; Pantos, G. D.; Sanders, J. K. M. *J. Am. Chem. Soc.* **2009**, *131*, 16030. (d) Coskun, A.; Saha, S.; Aprahamian, I.; Stoddart, J. F. *Org. Lett.* **2008**, *10*, 3187.
(26) (a) Vignon, S. A.; Jarrosson, T.; Iijima, T.; Tseng, H.-R.; Sanders, J. K. M.; Stoddart, J. F. *J. Am. Chem. Soc.* **2004**, *126*, 9884. (b) Iijima, T.; Vignon, S. A.; Tseng, H. R.; Jarrosson, T.; Sanders, J. K. M.; Marchioni, F.; Venturi, M.; Apostoli, E.; Balzani, E.; Stoddart, J. F. *Chem.—Eur. J.* **2004**, *10*, 6375. (c) Mullen, K. M.; Davis, J. J.; Beer, P. D. *New J. Chem.* **2009**, *33*, 769.
(27) (a) Talukdar, P.; Bollot, G.; Marenda, J.; Sakai, N.; Matile, S. *J. Am. Chem. Soc.* **2005**, *127*, 6528. (b) Hagihara, S.; Gremaud, L.; Bollot, G.; Mareda, J.; Matile, S. *J. Am. Chem. Soc.* **2008**, *130*, 4347.
(28) (a) Bhosale, R.; Míšek, J.; Sakai, N.; Matile, S. *Chem. Soc. Rev.* **2010**, *39*, 138. (b) Röger, C.; Mueller, M. G.; Lysetska, M.; Miloslavina, Y.; Holzwarth, A. R.; Würthner, F. *J. Am. Chem. Soc.* **2006**, *128*, 6542. (c) Röger, C.; Miloslavina, Y.; Brunner, D.; Holzwarth, A. R.; Würthner, F. *J. Am. Chem. Soc.* **2008**, *130*, 5929. (d) Sakai, N.; Sisson, A. L.; Bürgi, T.; Matile, S. *J. Am. Chem. Soc.* **2007**, *129*, 15758. (e) Sakai, N.; Bhosale, R.; Emery, D.; Mareda, J.; Matile, S. *J. Am. Chem. Soc.* **2010**, *132*, 6923. (f) Bhosale, S.; Sisson, A. L.; Talukdar, P.; Fürstenberg, A.; Banerji, N.; Vauthey, E.; Bollot, G.; Mareda, J.; Röger, C.; Würthner, F; Sakai, N.; Matile, S. *Science* **2006**, *313*, 84.
(29) Molla, M. R.; Das, A.; Ghosh, S. *Chem.—Eur. J.* **2010**, *16*, 10084.

(30) See the Supporting Information for detail.

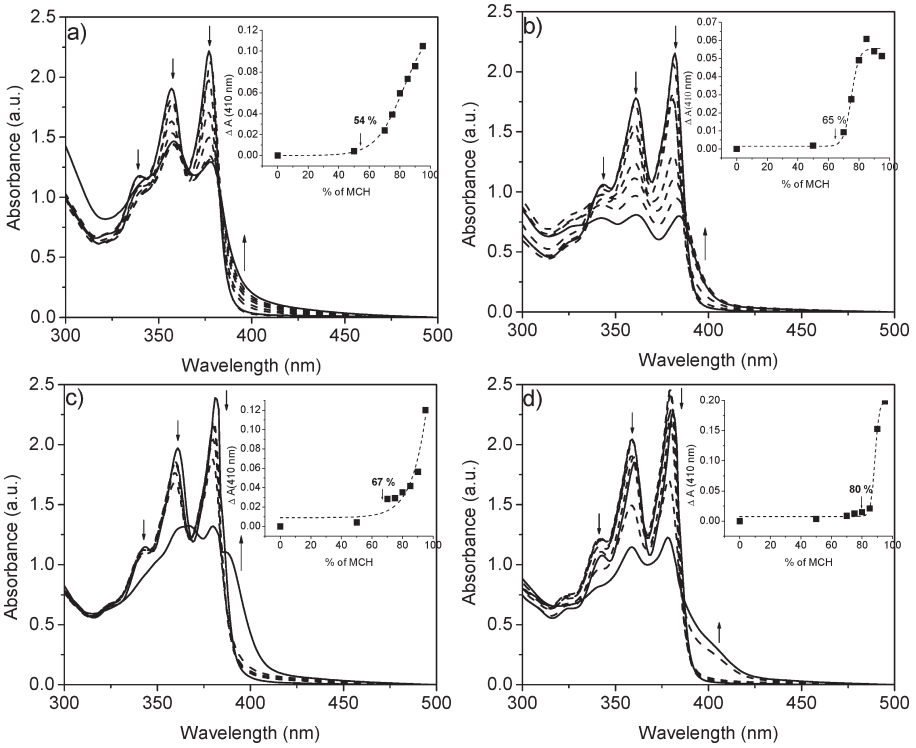

Figure 1. Solvent-dependent UV−visible studies of (a) **NDI-0**, (b) **NDI-2**, (c) **NDI-3**, and (d) **NDI-4**. Insets show the variation of Δ A at 410 nm as a function of solvent composition. Arrows indicate the spectral changes going from $CHCl_3$ to MCH. Temperature and concentration were maintained at 25 °C and 0.1 mM for each experiment.

shoulder in the absorption spectra at 410 nm in each case as a function of solvent composition. In the inset of each figure in Figure 1 we plot the ΔA ($A - A_0$) as a function of solvent composition where A and A_0 are the absorbance at 410 nm for particular composition of solvent and in $CHCl_3$, respectively. The inflection point of these plots (indicated by arrow in the inset) was taken as the critical solvent composition (CSC) for the onset of aggregation in each individual case and the values are reported in Table 1. It can be seen that the CSC values follow a regular trend in the order **NDI-0** < **NDI-2** < **NDI-3** < **NDI-4**, suggesting a decrease in the propensity of self-assembly with increasing distance of the amide-functionalities from the chromophore. This can be attributed to the increased hydrophobicity going from **NDI-0** to **NDI-4** due to the presence of a higher number of methylene segments, which helps them to tolerate a higher amount of MCH in the monomeric form.

Further to compare their thermal stability we carried out variable-temperature UV−visible studies (Figure 2) of individual chromophore in MCH/$CHCl_3$ (95:5) where at ambient temperature all of them form self-assembled structure. To our surprise, we observed that there was almost no spectral change in case of the **NDI-0** even when the temperature of the solution was raised to 65 °C (Figure 2a and its inset) suggesting considerably high thermal stability of its self-assembled structure. As no spectral changes were observed even at higher temperature, to eliminate the possibility of any irreversible structural conversion, we examined the effect of MeOH, a hydrogen-bonding competing solvent, on the UV−visible spectrum of **NDI-0** in MCH/$CHCl_3$ (95:5) and observed almost complete conversion of aggregate to monomeric species (see Figure S1 in the Supporting Information) in the presence of even 2% (v/v) of MeOH, clearly indicating the strong influence of H-bonding interaction in the self-assembly process and reversibility.[32] However, variable-temperature UV−visible experiments with the rest of the NDI derivatives revealed distinct spectral changes at higher temperature which clearly suggest reversible conversion of the self-assembled structure to the monomeric chromophores. With increasing temperature, absorption bands of the **NDI-2** and **NDI-3** showed gradual hyperchromic shift with concomitant blue shift, whereas in the

(31) Contrastingly for **NDI-4**, instead of red-shift, a blue shift of ~ 3 nm was observed for the lowest energy absorption band at 376 nm as a result of aggregation along with the appearance of a new shoulder band at around 403 nm. This probably indicates slightly different chromophore packing during self-assembly in this case compared to the other systems. Although the extent of spectral changes is significant in all cases and there should not be any doubt regarding the π-stacking, the assignments of J-type aggregates based on these changes may raise a question mark. In this context, it is noteworthy that very similar spectral changes for the same NDI chromophore has been indeed assigned as J-aggregate in recent literature (see ref 24). As our results corroborate well with the literature report, we assign the type of aggregates accordingly. However, it should be remembered that the extent of spectral changes in a specific type of aggregate depends on various parameters such as slip angle, center-to-center distance, and extent of rotational displacement, if any, of the two adjacent chromophores in the aggregated state.

(32) Similarly, we also carried out MeOH addition experiment to examine the existence of H-bonding in other NDI derivatives and observed in every case the self-assembled structure could be reverted to the monomeric chromophore in presence of 2−5% MeOH (see Figure S1 in the Supporting Information).This results of this experiment are strong evidence that H-bonding plays the crucial role in self-assembly.

Table 1. Solvent and Temperature-Dependent Self-Assembly Data and IR-data Revealing N−H Stretching Frequencies of Various NDI Derivatives

NDI derivative	CSC (MCH/$CHCl_3$) (%)	α_{50} T (°C)	IR stretching frequency (N−H bond) (cm^{-1})
NDI-0	54	>65	3228
NDI-2	63	64	3256
NDI-3	67	60	3260
NDI-4	80	54	3266

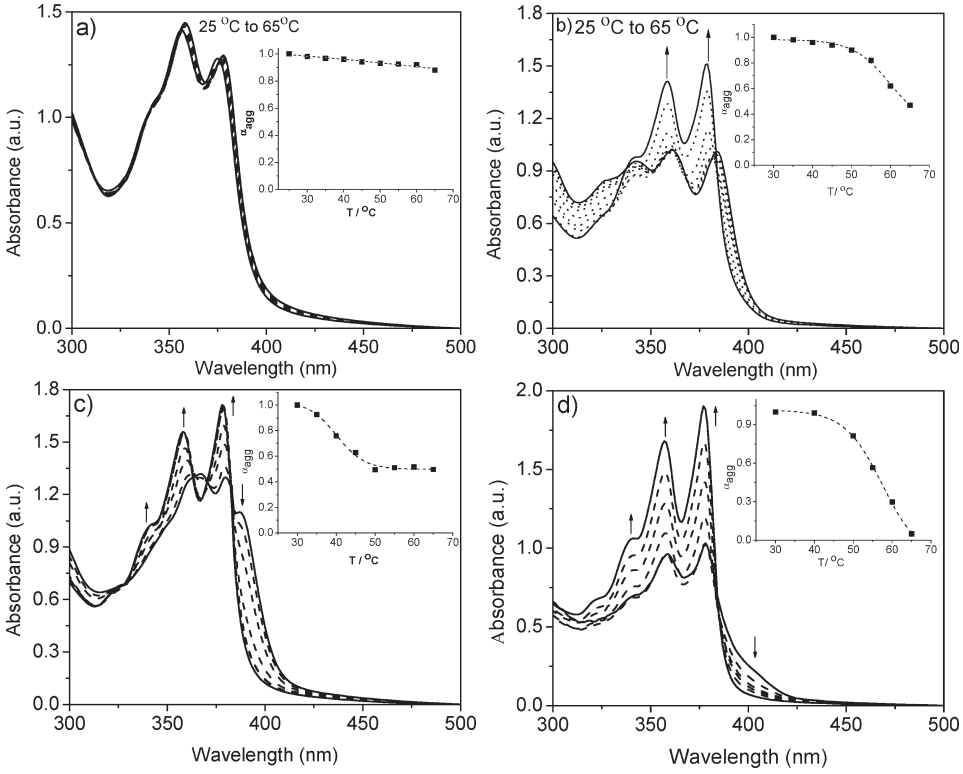

Figure 2. Variable-temperature UV−visible studies of (a) **NDI-0**, (b) **NDI-2**, (c) **NDI-3**, and (d) **NDI-4** in MCH/$CHCl_3$ (95: 5) solvent mixture at 0.1 mM concentration. Insets show the variation of mole fraction of aggregates with increasing temperature. Arrows indicate the spectral changes going from 25 to 65 °C.

case of **NDI-4**, a slight red shift of 2 nm was observed along with disappearance of the shoulder band which are in accordance with the solvent-dependent studies. From the variable-temperature absorption spectra the $\alpha_{50}(T)$ (temperature at which $\alpha_{agg} = 0.5$) values were calculated in each case using eq 1.[16a]

$$\alpha_{agg}(T) \approx \frac{A(T) - A_{mon}}{A_{agg} - A_{mon}} \qquad (1)$$

Where $\alpha_{agg}(T)$ is the mole fraction of aggregate at temperature T, A_{mon}, $A(T)$, and A_{agg} are the absorbance at 376 nm for the monomer (the value was taken from the absorption spectrum of the solution in $CHCl_3$), the solution at temperature T, and the pure aggregate solutions, respectively. The $\alpha_{agg}(T)$ values were plotted as a function of temperature in the inset of each figure in Figure 2 and from such a plot the $\alpha_{50}(T)$ were estimated separately in each case (Table 1). One would notice that the nature of the inset plot is different for **NDI-3** compared to **NDI-2** and **NDI-4** which is probably related to the distinctly different spectral changes along with most pronounced red-shift in case of **NDI-3** compared to the other two chromophores. However, from Table 1, it is clearly seen that the thermal stability of the various self-assembled structures as indicated by their respective $\alpha_{50}(T)$ follow a regular trend in the order **NDI-0** ≫ **NDI-2** > **NDI-3** > **NDI-4**. It is conceivable that as the distance between the amide-functionality and the chromophore increases the system become more flexible and thus bringing them to ordered self-assembled structure by hydrogen-bonding interaction will be associated with relatively more loss of entropy. However, that argument alone does not explain the unusually high thermal stability of **NDI-0** compared to other systems. To elucidate more on this, we examined the IR spectra of the xerogel of various NDI derivatives and compared the N−H stretching frequencies of the −NH−CO− functionality in each case (Figure 3, Table 1) which followed the order as **NDI-0** ≪ **NDI-2** < **NDI-3** < **NDI-4**, clearly revealing the difference in the strength of the hydrogen-bonding interaction. It is noteworthy that the N−H stretching frequency for **NDI-0** was 3228 cm^{-1}, which is significantly lower compared to the other three systems suggesting much stronger hydrogen bonding interaction in case of **NDI-0**. This can be attributed to the electron-withdrawing effect (−*I*) of the acceptor-type imide ring which is most influential for **NDI-0** due to the closest proximity and then gradually decreases as the distance increases. However, the difference in N−H

stretching frequencies among **NDI-2**, **NDI-3**, and **NDI-4** are not very significant which suggests that the strength of the H-bonding is not very different in these chromophores. Form the forgone discussions, it is evident that all the four NDI derivatives form self-assembled structure in nonpolar solvent because of π-stacking and H-bonding and the propensity for self-assembly follows the order **NDI-0** $\gg$ **NDI-2** $>$ **NDI-3** $>$ **NDI-4**.

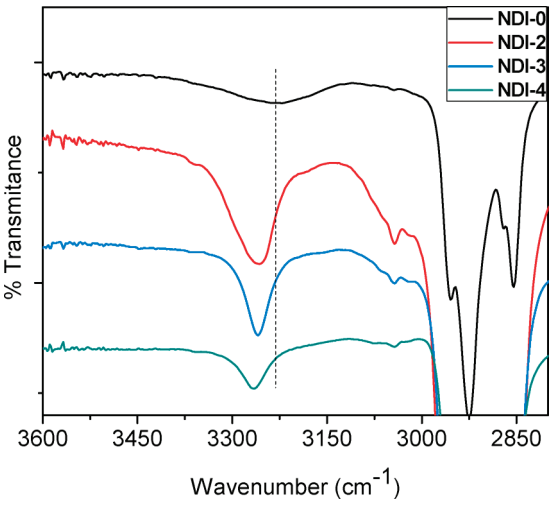

Figure 3. Selected region of the IR spectra of xerogel of various NDI derivatives showing the variation in the position of the band due to the N−H stretching of the amide functionality.

AFM Studies. To realize the effect of such distinct differences in solution behavior on the morphology of the self-assembled structure we examined their atomic force microscopic (AFM) images (Figure 4, Table 2). To our surprise, we found remarkable differences in the morphology of the various self-assembled structures. AFM-images of **NDI-0** revealed formation of self-assembled structure with short-range order wherein the average height of the fibers was found to be 6.7 ± 0.3 nm. On the other hand, **NDI-2** formed highly entangled micrometer long nanowires of nearly uniform nature with average height and width of 36.0 ± 0.3 nm and 140.8 ± 0.5 nm, respectively.

Moving from **NDI-2** to **NDI-3**, the morphology again changed drastically and instead of nanowires we observed distinctly different nanoribbons with much higher aspect ratio (average width was found to be 834.4 ± 0.5 nm, which is almost six times higher compared to that for **NDI-2**).[33] In this case, the extent of entanglement also appeared to be relatively less compared to **NDI-2**. For **NDI-4**, relatively flexible nanofibers were observed with signature of frequent rupturing along a single fiber. Critical analysis revealed a direct correlation of such diverse morphologies to the solution self-assembly behavior of the individual system. Much stronger H-bonding interaction in case of **NDI-0** as revealed by UV−visible and IR studies contributed to form extremely rigid self-assembled structure which probably prefers "mesophase"-like structure

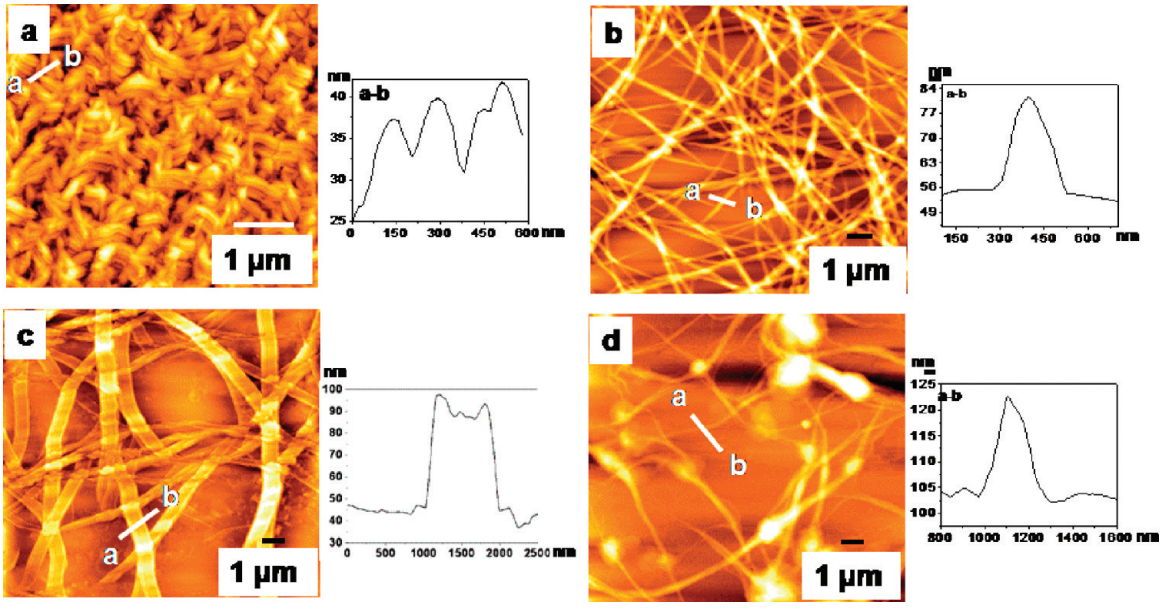

Figure 4. AFM height images (and cross-sectional analysis form a-b in each image) of dilute solutions of (a) **NDI-0**, (b) **NDI-2**, (c) **NDI-3**, and (d) **NDI-4** in MCH/$CHCl_3$ (95:5).

Table 2. Summary of AFM and Rheological Data for Various NDI Derivatives

sample/properties	height (AFM) (nm)	width (AFM) (nm)	G' (Pa)	$G' - G''$ (Pa)	σ_y (Pa)
NDI-0	6.7 ± 0.3	82.0 ± 1	[a]		
NDI-2	36.0 ± 0.3	140.8 ± 0.5	29 900	26 395	298
NDI-3	39.2 ± 0.4	834.4 ± 0.5	1649	1365	16
NDI-4	18.0 ± 0.1	142 ± 1	698	600	13

[a] No gelation was observed in this case.

formation. It is noteworthy that for a related perylene system Würthner and co-workers have recently reported formation of chromonic mesophases and absence of any elongated structure formation.[34] For **NDI-2** and **NDI-3** formation of elongated fiber is facilitated by optimum balance between the self-assembly and flexibility, which is provided by the presence of methylene groups in-between the chromophore and the amide functionalities. Although both of them form J-type aggregate, there chromophoric arrangement are not same as evident from the difference in their spectral shift as a result of self-assembly (Figure 1b,c). A much larger red shift was observed in the case of **NDI-3** compared to **NDI-2** probably suggesting significant difference in their relative longitudinal displacement along the long axis and thus the slip angle as well as the center-to-center distance between the two adjacent chromophores during self-assembly. It may be possible that due to these differences the **NDI-3** stacks with stair-case like structure accumulating more space per single stack and thus the resulting higher-order structure adopts the ribbonlike morphology. Contrary to this, **NDI-2** forms more compact stacks with relatively less cross-sectional volume in the space and consequently it generates wirelike nanostructures. For **NDI-4**, we already have observed a signature of relatively weak self-assembly in their solution photophysical behavior, which inhibits formation of elongated nanostructure as observed in case of **NDI-2** or **NDI-3**, and thus frequent discontinuity in their AFM images was observed.

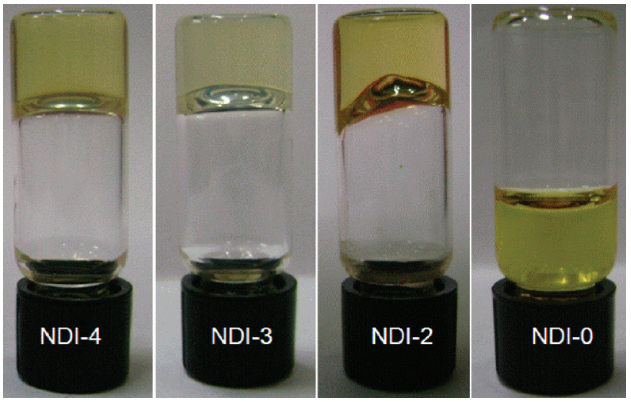

Figure 5. Pictures of the gel/sol formed by various NDI derivatives in cyclohexane at 1.5 mM concentration.

Gelation Study. We envisaged that the versatile morphologies of this series of NDI-derivatives would play crucial role in their gelation behavior. To check this, we studied the gelation of all four compounds in few common organic solvents (see the Supporting Information, Table S1). To our surprise, we found that the most strongly aggregated **NDI-0** failed to induce gelation in any of the tested solvents and remained soluble in all those cases even at relatively high concentration (10 wt %). On the other hand **NDI-2**, **NDI-3**, and **NDI-4** all showed gelation ability (Figure 5).

This clearly suggests that formation of strong self-assembled structure is not the only criteria for gelation but the morphology of the self-assembled structure and its interaction with the solvent molecules also play crucial role in gel-formation. From the AFM images of **NDI-0**, it is obvious that they do not form long enough fibers required for gelation. Instead, they showed formation of aggregates with short-range crystallike order, which is probably the reason that they still maintain the liquidlike mobility even in the self-assembled state. To understand more about this intriguing nature of the self-assembly in this particular case, we examined the phase properties of a solution of **NDI-0** in cyclohexane at 2.0 wt % solution using an optical polarized microscope (OPM), which indicated the presence of only isotropic phase. Subsequently, we increased the concentration and examined the OPM images of 10 wt % solutions and in this case we observed distinct Schlieren texture (Figure 6), which is indicative of formation of a chromonic nematic (N) phase that is a special type of lyotropic mesophase formed by disk-shaped mesogens.[35] In the N phase, the mesogens stack to form columns without any positional order. We further examined the effect of shearing on these structures; from Figure 6, it is evident that the texture could be recovered after shearing. When the solution was allowed to edge-evaporate between two cross-polarizers, formation of grainy texture was observed, which indicates hexagonal arrangements of the columns in chromonic M phase.[35a] The subject of chromonic LC phases is still not well understood and it is believed that formation of such mesophase is an enthalpy-driven process.[35d,35e] Thus it is possible that the most pronounced H-bonding interaction in **NDI-0** compared to the other chromophores in this

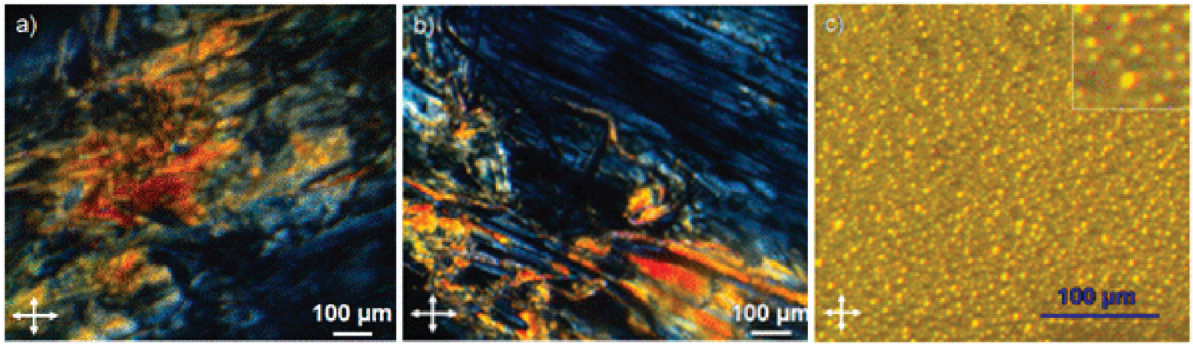

Figure 6. Representative optical textures of **NDI-0** in cyclohexane solution (10 wt %) as observed under crossed polarizers of a optical microscope: (a) Schlieren texture for a N phase; (b) recovered texture after shearing; (c) grainy textures of M phase after the film was concentrated by edge evaporation for 3 h inset showing the zoomed region from (c). The double arrows indicate the configurations of the polarizers.

series contributes to formation of this particular type of self-assembled structure. It is noteworthy that to date, formation of chromonic mesophase has been restricted to being mostly in aqueous medium and there are only few reports[35f] that include highly polar solvents like DMF and MeOH in which such a mesophase formation has been observed. But to best of our knowledge, there is only one report wherein Würthner and co-workers have demonstrated[34] chromonic mesophase formation in highly nonpolar solvent cyclohexane like in the present study. Chromonic mesophases have already gained enough attention because of the possibility of them utilized in various materials-related applications and we believe the present serendipitous discovery will add significantly to logical design of functional building blocks which will exhibit such self-assembly properties.

NDI-2 and **NDI-3** formed a gel in the maximum number of solvents, which includes aliphatic hydrocarbon (cyclohexane, methylcyclohexane) and nonpolar chlorinated solvents (tetrachloroethylene, carbon-tetrachloride), because of strong self-assembly and the formation of elongated fibers as revealed by AFM images. However, for **NDI-4**, gelation was observed only in aliphatic hydrocarbon solvents. This is because in this case, the self-assembly was found to be already weak in hydrocarbon-like solvents and thus it is expected to be even weaker in chlorinated solvents. To confirm this, we probed the self-assembly of **NDI-4** in tetrachloroethylene (TCE), a chlorinated nonpolar solvent and found that going from $CHCl_3$ to TCE, the absorption spectra remained almost unchanged, suggesting that in this case there was no self-assembly, which explains why no gelation was observed for **NDI-4** in chlorinated solvents. It may be argued that the gelation is studied in pure cyclohexane, whereas the AFM was examined from dilute solution of the samples in $MCH/CHCl_3$ (95:5). To examine the effect of this minor variation in the solvent system, we also studied the AFM images of **NDI-2** in pure cyclohexane itself as a case study and found identical morphology (see Figure S3 in the Supporting Information) to that observed in the mixed solvent.[30]

Rheological Studies. We examined the flow behavior of the gels (**NDI-2**, **NDI-3**, and **NDI-4**) by studying their rheological properties in cyclohexane gel (1.9 wt %).[36] In a typical stress−amplitude sweep measurement, we monitored the variation of storage modulus (G') and loss modulus (G'') as a function of applied stress (Figure 7) and the relevant data from these experiments are presented

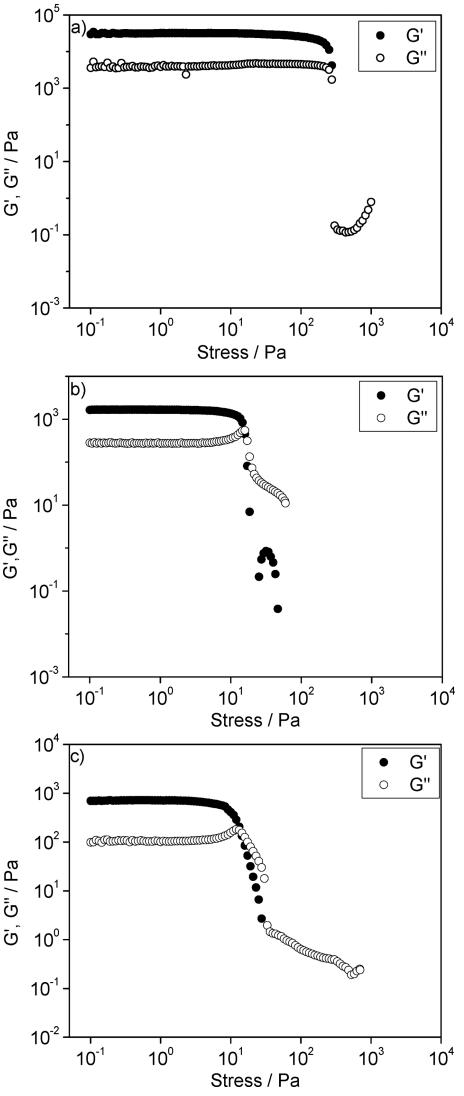

Figure 7. Variation of the elastic modulus (G') and the viscous modulus (G'') as a function of applied stress for 1.9 wt % gels of (a) **NDI-2**, (b) **NDI-3**, and (c) **NDI-4** in cyclohexane at 25 °C. As the Y axis is in the log plot, few negative data are not shown.

in Table 2. It is noteworthy that G' and G'' represent the ability of a deformed material to resume its original shape and tendency of a material to flow, respectively.

For an ideal liquid, $G' = 0$, and for an ideal solid, $G'' = 0$. In Figure 7, it can be seen that for all the three gelators initially $G' > G''$ suggesting existence of "solid-like" gel phase.[37] As the applied stress was increasing, both G' and G'' remained almost invariant until a certain point wherein always $G' > G''$. The difference in these two moduli ($G' - G''$) is considered to be a measure of the dominance of the elastic behavior of the material over its viscous properties and in the present series that followed the order **NDI-2** ≫ **NDI-3** > **NDI-4** (Table 2). From **NDI-4** to **NDI-3**, this difference increased only by a factor of 2, which can be attributed to their difference in the strength of self-assembly. For **NDI-2,** the difference reached a remarkably high value of ∼30 000 Pa, which is 18 times higher than that of **NDI-3** indicating much superior

(33) For a recent report on formation of such versatile morphologies of oligo-aniline system, see: Wang, Y.; Tran, H. D.; Liao, L.; Duan, X.; Kaner, R. B. *J. Am. Chem. Soc.* **2010**, *132*, 10365.
(34) Li, X. Q.; Zhang, X.; Ghosh, S.; Würthner, F. *Chem.—Eur. J.* **2008**, *14*, 8074.
(35) (a) Tam-Chang, S. W.; Helbley, J.; Iverson, I. K. *Langmuir* **2008**, *24*, 2133. (b) Tam-Chang, S. W.; Huang, L. *Chem. Commun.* **2008**, 1957. (c) Lydon, J. *Curr. Opin. Colloid Interface Sci.* **2004**, *8*, 480. (d) Lydon, J. *Curr. Opin. Colloid Interface Sci.* **1998**, *3*, 458. (e) Chami, F.; Wilson, M. R. *J. Am. Chem. Soc.* **2010**, *132*, 7794. (f) Smirnova, A. I.; Bruce, D. W. *Chem. Commun.* **2002**, 176.
(36) Sollich, P. *Molecular Gels: Materials with Self-Assembled Fibrillar Networks*; Weiss, R. G.; Terech, P., Eds.; Springer: Dordrecht, The Netherlands, 2006; Chapter 5.
(37) Menger, F. M.; Peresypkin, A. V. *J. Am. Chem. Soc.* **2003**, *125*, 5340.

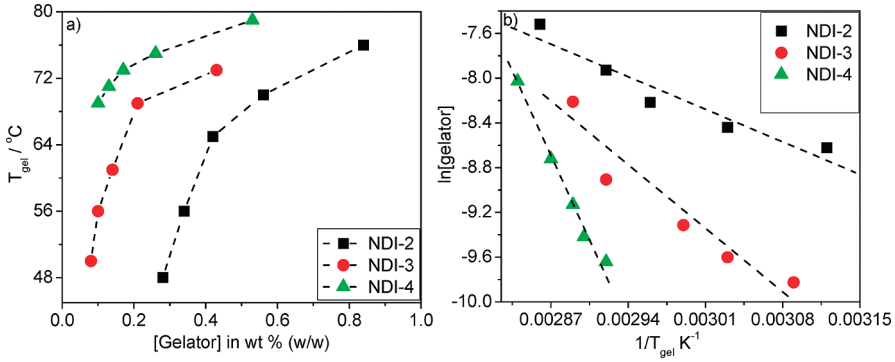

Figure 8. (a) Variation in T_g with concentration for various NDI derivatives; (b) plot of ln [gelator] vs $1/T_g$ for determination of the ΔH_m using Schroeder−van Laar equation.

Table 3. ΔH_m and CGC Values for Various NDI Gelators

NDI derivative	ΔH_m (KJ)	CGC (MCH) (wt %)	CGC (cyclohexane) (wt %)	CGC(CCl4) (wt %)	CGC (TCE)
NDI-2	35.26	0.17	0.17	0.02	0.06
NDI-3	62.27	0.10	0.069	0.16	0.11
NDI-4	172.57	0.19	0.11	[a]	[a]

[a] No gelation was observed in this case.

elastic property compared to the other two gelators.[38] However beyond a certain amount of applied stress, G' and G'' deviated from the linearity and crossed eachother. The stress at which this crossover point is reached is defined as the yield-stress (σ_y), which represents robustness of a particular gel system. σ_y values for **NDI-3** and **NDI-4** were almost comparable, with a slightly higher value in the former case indicating marginally higher robustness compared to **NDI-4**. However, for **NDI-2**, the σ_y value was estimated to 298 Pa, which is again 18 times higher than that of **NDI-3,** reiterating its unparallel resistance against flow when compared to the other two gelators. The remarkably different and superior viscoelastic properties for **NDI-2** are extremely surprising particularly if one considers the fact that the only structural difference between **NDI-2** and **NDI-3** is the presence of one additional methylene group in between the chromophore and the amide functionality. It can also be recalled that the strength of the self-assembly as revealed by the $\alpha_{50}(T)$ values were not so different between **NDI-2** and **NDI-3** that one can anticipate such highly contrasting flow behavior for that reason alone. Thus we propose it is not only the strength, but the morphology of the self-assembled structure which plays most critical role in determining the gel properties. We have already discussed vast differences in the morphologies of **NDI-2** and **NDI-3**. Althogh the AFM images of the former systems showed presence of uniform nanowires, the latter showed distinctly different ribbonlike structure with less entanglement. We believe these differences in the morphology contribute most significantly to determining the viscoelastic properties of the resulting gels and thus they differ to such a large extent.

Determination of Thermodynamic Parameters. The enthalpy of melting (ΔH_m) of the gel-to-sol transition was estimated using Schroeder−van Laar equation (eq 2).[39]

$$\ln c = \frac{\Delta H_m}{RT_g} + \text{constant} \qquad (2)$$

Where R is the universal gas constant and T_g is the gel-to-sol melting temperature at concentration c. To understand the effect of the structural variation in the building block of the present NDI gelator series on the ΔH_m values of the corresponding gels, we determined the same for all the three gelators. To do so, first T_g were determined for **NDI-2**, **NDI-3**, and **NDI-4** and with increasing gelator concentrations exponential increase of T_g was observed in all three cases (Figure 8a). Utilizing these data we made Arrhenius plot of ln c vs $1/T_g$ and as expected linear plots were observed in all three cases (Figure 8b).

From the slope of these plots ΔH_m values were calculated using eq 2 and the values are presented in Table 3. We found that the ΔH_m values follow the order **NDI-4** > **NDI-3** > **NDI-2**, which can be attributed to the enhanced hydrophobicity of the gelator with increasing number of methylene units and corroborate well with the solvent dependent UV−visible studies.[39] Further with increasing number of methylene units in between the chromophore and the amide functionality, the flexibility of the fibers also increases, which may allow for better interaction of the self-assembled fibers with the nonpolar solvent.

This also explains the trend observed in the critical gelation concentration (CGC) of the three gelators (Table 3). In general the CGC values were found to be < 0.2 wt % in all cases, which indicates a very efficient gelation ability for all the gelators. Particularly for **NDI-3**, the CGC

(38) Nguyen, M. K.; Lee, D. S. *Chem. Commun*. **2010**, *46*, 3583.

(39) (a) Raghavan, S. R.; Cipriano, B. H. *Molecular Gels: Materials with Self-Assembled Fibrillar Networks* Weiss, R. G.; Terech, P., Eds.; Springer: Dordrecht, The Netherlands, 2006, Chapter 8. (b) Das, U. K.; Trivedi, D. R.; Adarsh, N. N.; Dastidar, P. *J. Org. Chem*. **2009**, *74*, 7111. (c) Abdallah, D. J.; Lu, L.; Weiss, R. G. *Chem, Mater* **1999**, *11*, 2907. (d) Abdallah, D. J.; Weiss, R. G. *Langmuir* **2000**, *16*, 352.

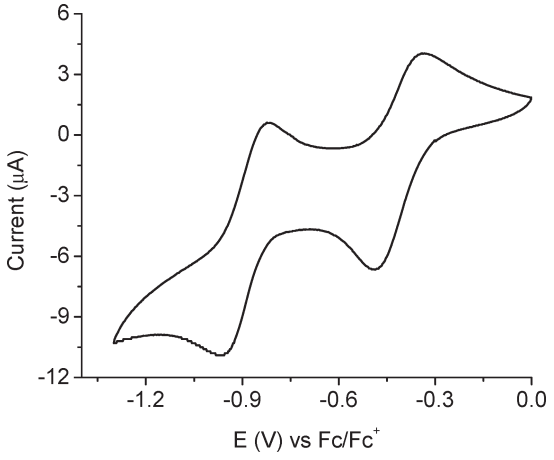

Figure 9. Cyclic voltammogram for **NDI-0**. Internal reference electrode, ferrocene; scanning rate, 50 mV/sond; temperature, 25 °C.

Table 4. Redox Potentials and LUMO Energy Levels of NDI Derivatives from Cyclic Voltametry Measurements

NDI derivative	E_0-E_{-1} (V)[a]	$E_{-1}-E_{-2}$ (V)[b]	$E_{average}$ (V)[c]	LUMO[d] (eV)
NDI-0	−0.41	−0.88	−0.64	−3.76
NDI-2	−0.46	−0.86	−0.66	−3.75
NDI-3	−0.47	−0.89	−0.68	−3.73
NDI-4	−0.53	−0.94	−0.73	−3.67

[a] First reduction potential. [b] Second reduction potential. [c] Average of the first and second reduction potentials. [d] $E_{LUMO} = -e(E_{1/2(redox)} - E_{Fc} + 4.8)$; $E_{Fc} = 0.39$ V (versus Ag/AgCl).

values were very low and in one case it was even less than 0.1 wt %, which qualifies it to be called as "Supergelator" according to conventional practice.[16a] Formation of elongated and thermally stable fiber depends upon the propensity of self-assembly, whereas we found the interaction of the gel fibers with the solvent molecules is also influenced by the hydrophobicity and flexibility. For **NDI-3**, the optimal balance of these two parameters is achieved and thus it shows such low CGC values. However, in chlorinated solvent, the CGC of **NDI-2** was found to be less than that of **NDI-3**, suggesting in this case the propensity of self-assembly probably takes the dominating role in determining the CGC.

Cyclic Voltametry (CV) Analysis. The redox properties of all the four NDI derivatives were studied by CV measurements using Pt electrode as working as well as counter electrode, Ag/AgCl electrode as reference electrode and tetrabutylamonium perchlorate (0.1 M) as supporting electrolyte. Solutions of the NDI derivatives were made in dichloromethane solvent (1 mM) for these measurements. A representative cyclic voltammogram (for **NDI-0**) is shown in Figure 9 and it can be seen that there are two reversible reduction waves due to the formation of radical anions and dianions. Very similar observations were made for rest of the NDI derivatives (see the Supporting Information for detail). The CV data are summarized in Table 4 and it can be noticed that the average reduction potential varies from −0.64 to −0.73 V vs Fc/Fc^+ (Fc: ferrocene) and the corresponding LUMO energy varies from −3.76 to −3.67 eV. It is also noteworthy that no oxidation was observed up to 1.8 V. These results are in accordance with literature report[40] and suggest the n-type semiconducting nature of the NDI chromophores.

Conclusions

In this paper, we have shown remarkable effect of a simple structural variation on the self-assembly, morphology, mesophase formation and gelation of a series of bis-(trialkoxy-benzamide) functionalized n-type semiconducting NDI chromophores. Number of methylene units (n) in-between the amide functionality and the NDI ring was adjusted to 0, 2, 3, 4 and we found in all these cases self-assembly was achieved in nonpolar solvents due to the synergistic effect of π-stacking and hydrogen-bonding. However, the stability and chromophore-packing pattern of the self-assembled structure were found to be greatly dependent on the value of n. With increasing n, the propensity of self-assembly decreased continuously. Morphology of the self-assembled structure was found to be dictated by n and we observed formation of short-length aggregates with crystal-like order for $n = 0$; highly entangled micrometer-long nanowires for $n = 2$; relatively less-entangled nanoribbons with much higher aspect ratio for $n = 3$ and discontinuous hairy nanofibers for $n = 4$. The effect of such vastly different morphologies was clearly reflected in their macroscopic properties such as gelation. For $n = 2$, 3, and 4, gelation was observed in nonpolar organic solvents with case-dependent thermal stability, flow-behavior and thermodynamic parameters and all these aspects could be correlated to the strength of the self-assembly and morphology of the respective chromophores. Most striking differences was observed for the flow-behavior of the $n = 2$ and $n = 3$, wherein we observed extremely high value of yield stress for $n = 2$ compared to $n = 3$, which was attributed to their very different morphology (nanowires vs nanoribbons). However, much to our surprise, we found the most strongly aggregated NDI chromophore with $n = 0$ did not form gel in any of the tested solvents. Rather, it formed chromonic type lyotropic mesophases (possibly driven by enthalpy-related parameters), which has been rarely reported in organic solvents for any chromophores and there has not been any report for NDI chromophore. Redox properties of these chromophores were studied by cyclic voltametry and the results corroborate well with literature to indicate the n-type semiconducting nature of the NDI chromophore. Such a remarkable effect on the self-assembly due to this simple structural variation has been an eye-opening experience for us and we believe this study will certainly open up many exciting possibilities to precisely tune the photophysical properties, morphology, size, shape, and macroscopic properties of various other functional

(40) (a) Erten, S.; Alp, S.; Icli, S. *J. Photochem. Photobiol. A: Chem.* **2005**, *175*, 214. (b) Thalacker, C.; Röger, C.; Würthner, F. *J. Org. Chem.* **2006**, *71*, 8098. (c) Gawrys, P.; Djurado, D.; Rimarik, J.; Kornet, A.; Boudinet, D.; Verihac, J. M.; Lukeš, V.; Wielgus, I.; Zagorska, M.; Pron, A. *J. Phys. Chem. B* **2010**, *114*, 1803.

π-systems, which has enormous importance in advanced opto-electronic device applications.

Acknowledgment. We thank Department of Science and Technology (DST), New Delhi, India, for financial support (Project SR/FT/CS-039/2008). We also thank Mr. Pradip Ghosh of Department of Inorganic Chemistry, IACS, for the cyclic voltametry measurements.

Supporting Information Available: Synthesis and characterization, additional spectral data, CV data, gelation data, and AFM images (PDF). This material is available free of charge via the Internet at http://pubs.acs.org.